

On the choice of the weather dataset in hygrothermal simulations in Mediterranean climate: MRY vs TWY

Alessandra Urso¹, Vincenzo Costanzo¹, Gianpiero Evola², Francesco Nocera¹

¹ Department of Civil Engineering and Architecture (DICAR),
Università degli Studi di Catania, Via S. Sofia 64, Catania, Italy

² Department of Electric, Electronic and Computer Engineering (DIEEI),
Università degli Studi di Catania, Via S. Sofia 64, Catania, Italy

Abstract

The Standard EN ISO 15026:2007 suggests that, in Heat and Moisture Transfer (HAMT) simulations, a Moisture Reference Year (MRY) should be used, built upon a sufficiently long recording period. However, many studies rely on widely available Typical Weather Years (TWY), although these are not prepared *ad hoc* to investigate moisture-related risks. This paper aims at understanding to what extent these weather files are interchangeable in a warm climate, through hygrothermal simulations performed with Delphin 6.1.2 on a typical wall assembly retrofitted by wood-based materials. All tested weather files refer to the same location (Catania, Italy) and reference period. The results are compared in terms of mold growth and moisture-dependent increase in heat losses.

Highlights

- The “cold” MRY is the most conservative choice to assess the mold growth risk.
- All weather files provide very similar moisture-dependent U-values, which vary by just 1%.
- TMY and MRY can be interchangeable in Catania, since they provide the same degree of risk.
- The mould growth risk is strongly correlated with mean outdoor temperature and total wind driven rain.

Practical implications

The TWY-based simulations show results similar to MRY-based ones. This can justify the use of available and easily accessible TWY in the assessment of moisture-related risks – although they are not built *ad hoc* for hygrothermal simulations – at least for wall assembly and climate conditions similar to those addressed in this study.

Introduction

Numerical dynamic hygrothermal simulations are useful tools to predict moisture damage and performance decay in building components. Indeed, these analyses can provide a valid support to the design of innovative envelope solutions without a consolidate tradition, especially when they contain organic materials (wood, straw, cellulose) that are particularly prone to long-term moisture-related risks, such as mold growth. On the other hand, the development of highly performing building envelope components requires that heat losses are reduced, but this is in turn negatively influenced by the moisture accumulated within building materials. For these reasons,

advanced dynamic hygrothermal simulations are currently not only applied by the scientific community, but they are also becoming an indispensable tool for a conscious design and the diffusion of more sustainable technologies. For instance, HAMT simulations were used by Strang et al. (2021) to identify best-practice design solutions for Cross Laminated Timber (CLT) buildings, with the aim to support the fast uptake of this technology in hot and humid locations. Furthermore, Koh et Kraniotis (2021) investigated the hygrothermal and energy performance of straw bale buildings and found out that, when properly designed, they achieve a very low energy use and robust hygrothermal performance. Finally, Aversa et al. (2021) investigated the hygrothermal performance of hemp-lime buildings, and provided solid bases for developing future guidelines and enhancing the diffusion of this kind of technology.

Nevertheless, some methodological aspects of HAMT simulations still require further investigation, such as the selection of appropriate climate datasets to run reliable simulations. In particular, a reliable assessment should be able to predict the moisture behavior of the building components without an undue under- or over-estimation of the damage. In this regard, the Standard EN ISO 15026:2007 (CEN, 2007) suggests that a Moisture Reference Year (MRY) representative of the 90-th percentile conditions occurring in a long-term period has to be used. According to the Standard, the MRY should be prepared from weather data recorded over at least ten consecutive recent years, and following suitable procedures. However, such a series of weather data is not always available; thus, many studies based their hygrothermal simulations on Typical Weather Years (TWY) in place of MRYS, in contrast with the recommendations by the Standard (Brambilla et al, 2021; Martin-Garin et al, 2021; Zhu et al, 2022). The main difference between MRY and TWY is that the latter depicts an average climate trend that is suitable to assess the average energy performance, but it is not representative of those climate conditions that actually impact on the hygrothermal performance of building components, such as the wind driven rain: in other terms, a TWY is not built *ad hoc* to investigate moisture related-risks. However, since TWY codification dates back to some decades ago, when the scientific community started using dynamic building energy simulations, this type of weather file is currently largely used and easily accessible for many different locations worldwide.

In this framework, this paper aims to understand whether and to what extent the use of TWYs can be justified also in the assessment of the moisture-related risks, in place of an MRY. To this purpose, the paper discusses the results of a series of hygrothermal simulations based on several different MRYs prepared according to the Standard EN ISO 15026:2007, as well as on a TWY built according to the IWEC procedure for the same location and reference period (Catania, Italy, 2005 – 2019). The hygrothermal simulations refer to an innovative wood-based retrofit solution, developed within the H2020 project “e-SAFE” and applied to the envelope of a demonstration building located in Catania. The simulations are performed with the software Delphin 6.1.2 (Delphin®, 2021): this is one of the most used HAMT tools in the scientific community, developed at the Dresden University of Technology and complying with the Standard EN ISO 15026:2007. The results of the various simulations are compared by looking at both the mold growth risk and the increased thermal losses due to the moisture stored within materials.

Finally, the paper discusses possible correlations between the above moisture related risks and the mean monthly or annual weather conditions, to draw more general conclusions that might be applied to other climates.

Methodology

In this paper, HAMT simulations are carried out for the walls of a building located in Catania, Italy, supposing that the opaque vertical components are retrofitted through a solution called “e-CLT”. This retrofit solution is currently under development in the framework of the H2020 “e-SAFE” project, which aims to integrate seismic safety and energy efficiency during the building renovation stage. The e-CLT solution is here investigated because it is made of wood-based materials, i.e. CLT and wood-fiber insulation. Since wood is an organic material, it is more sensitive to decay caused e.g. by mold growth, and it is particularly prone to moisture storage due to its cellular structure (Evola et al, 2021).

More specifically, the retrofitted wall assembly is composed – from the internal to the external side – by the following layers: 20 mm of cement plaster, 80 mm of hollow concrete blocks, 100 mm of non-ventilated air cavity, 120 mm of hollow concrete blocks, 30 mm of cement plaster, 100 mm of cross laminated timber CLT, 60 mm of wood fiber, and an external cladding with a scarcely-ventilated air gap (20 mm) and a 12-mm thick cement board (Figure 1).

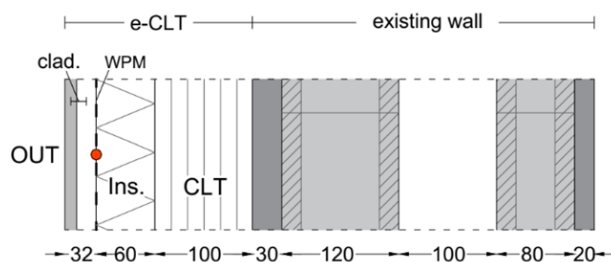


Figure 1: Stratigraphy of the wall under investigation

The e-CLT also includes a vapor-open water-proof membrane (WPM, $s_d = 0.04$ m) to protect the insulation layer from the effect of wind driven rain, applied to the external side of wood fiber. Materials are selected from the Delphin database (Vogelsang et al, 2013), by changing some properties in case of missing materials as reported in (Evola et al, 2022) The thermal conductivity of the air cavity is defined as an equivalent value calculated from their thermal resistance. Table 1 and Table 2 show the main thermal and hygroscopic properties of the selected materials.

Table 1: Thermal properties of the selected materials

Material	s mm	ρ kg/m ³	c_p J/(kg·K)	λ_{dry} W/(m·K)
Cement plaster	20	1390	850	0.75
Clay blocks	80	845	1000	0.29
Non-ventilated air gap	100	1.3	1050	0.56
Clay blocks	120	667	1000	0.39
Cement plaster	30	1390	850	0.75
CLT	100	450	1843	0.12
Wood Fiber (WF)	60	50	1000	0.04
Air cavity	20	1.3	1050	0.22
Cement board	12	1159	1188	0.60

Table 2: Hygroscopic properties of the selected materials

Material	μ -	A g/(m ² ·s ^{1/2})	θ_{80} kg/m ³	θ_{sat} kg/m ³
Cement plaster	33	30	40.7	430.0
Clay blocks (80 mm)	15	177	11.4	319.4
Non-ventilated air gap	1	0	0.0	1000.0
Clay blocks (120 mm)	15	177	11.4	319.4
CLT	186	5	59.8	728.1
Wood Fiber (WF)	1	5	12.7	590.3
Air cavity	1	0	0.0	1000.0
Cement board	26	14	70.9	283.6

The simulations are repeated for different climate datasets referring to the same location and reference period. In particular, weather data were recorded from 2005 to 2019 at the weather station of Sicilian Agrometeorological Information System (SIAS) located in Catania (latitude: 37.26°, longitude: 15.04°, elevation: 10 m a.s.l.). The missing recordings are integrated as reported in Costanzo et al. (2020). Starting from these weather data, three MRYs are built according to the instructions of the Standard EN ISO 15026:2007. Indeed, the Standard suggests three different criteria depending on which climate condition (i.e. low temperature, high temperature, or high rainfall) is likely to be the most critical one for the investigated moisture problems. Since this is not known *a priori*, all three possible MRYs are selected and used in this study.

In particular, Figure 2 shows the mean temperature (°C) and the total rainfall on a horizontal plane (mm/year) for each year of the reference period, arranged in rising order.

Thus, according to the Standard, the year with the mean temperature closest to the 10-th percentile of the distribution is chosen as “COLD” year, the year with the mean temperature closest to the 90-th percentile is chosen as “HOT” year, while the year with the total rainfall closest to 90-th percentile is identified as “RAINY” year. Then, a TWY is built according to the IWEC procedure as described in Costanzo et al. (2020). Thus, Figure 2 also reports the mean temperature and the total rainfall for this typical year, and compares this climate dataset to the three selected MRYs.

As expected, if looking at the air temperature the TWY reflects the average behavior of the 15 years considered. In fact, the mean air temperature in the TWY is 18.1 °C and is in between the 10-th percentile (17.4 °C) and the 90-th percentile (18.6 °C) of the entire distribution. On the contrary, its total rainfall (900 mm) is slightly above the 90-th percentile of the reference period (840.5 mm). This happens because the IWEC, as well as other procedures for building typical weather years (e.g., TMY2, TMY3, ISO), select months taken from different years, without taking the rainfall into account. Thus, the high amount of rainfall is probably related to a casual concatenation of rainy months, which suggests a first possible limitation of using a TWY in HAMT simulations: indeed, a non-realistic rainfall value could severely impact on the moisture performance. For this reason, further considerations about the role of rainfall, temperature and relative humidity, are provided in the Discussion section.

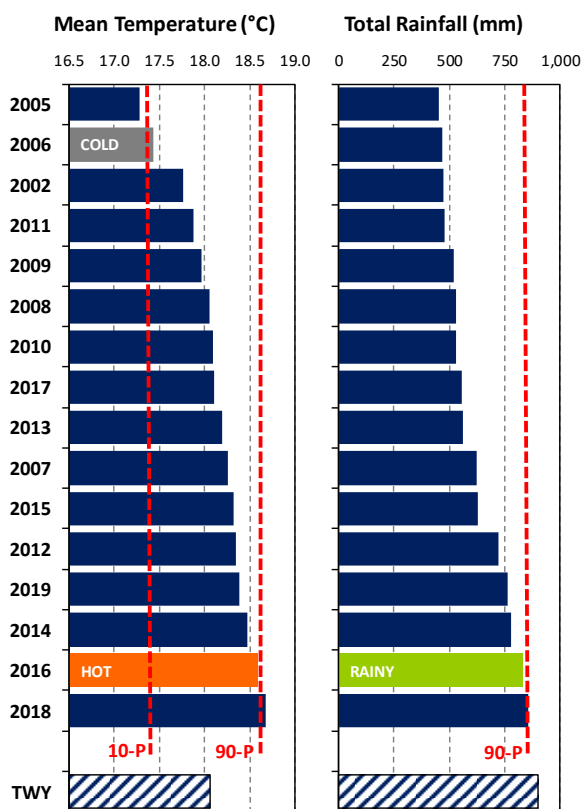


Figure 2: Comparison among the selected years, aimed to select the Moisture Reference Year.

Left: mean annual temperature; right: total annual rainfall

The simulations consider also four different wall orientations (North, East, South, and West). This is particularly relevant when dealing with the wind-driven rain (WDR), calculated by Delphin according to the Standard EN ISO 15927-3 (CEN, 2009) by using a reduction coefficient of 0.7 to include the rain splashing effect (Urso et al, 2022). Furthermore, a water source is assigned to the outer surface of the insulation layer protected by the WPM: this is set to 1% of the rain flux incident on the external surface, and is measured in $\text{kg}\cdot\text{m}^{-2}\cdot\text{h}^{-1}$. This approach is adopted by several studies in compliance with the recommendations of the ASHRAE 160 Standard (ASHRAE, 2016) and allows simulating a rain leakage through the cladding (Chang et al, 2020; Wang et al, 2020). The hourly data for the rain leakage is obtained by preliminary simulations and by requiring as an output the rain flux normal to the external surface.

As far as the outdoor boundary conditions are concerned, the outside heat transfer coefficient and surface vapor diffusion coefficient are set to $25 \text{ W}\cdot\text{m}^{-2}\cdot\text{K}^{-1}$ and $7.5\cdot 10^{-8} \text{ s}\cdot\text{m}^{-1}$, respectively. The solar absorption coefficient is set to 0.6 and the long wave emissivity is set to 0.9 (default values). The indoor climate conditions are defined according to the Standard EN ISO 15026 (CEN, 2007), and consider the variation in indoor air temperature and relative humidity as a function of outdoor conditions: the indoor air temperature is allowed to range from 20 °C to 25 °C, and the relative humidity from 35% to 65%. The inside heat transfer coefficient and surface vapor diffusion coefficient are set to $8 \text{ W}\cdot\text{m}^{-2}\cdot\text{K}^{-1}$ and $2.5\cdot 10^{-8} \text{ s}\cdot\text{m}^{-1}$.

In order to reach a stabilized behavior, simulations are performed over 10 consecutive years and by assuming as initial conditions for all construction materials $T = 20 \text{ °C}$ and $\text{RH} = 80\%$. Before running the simulations, the assemblies are discretized in 145 smaller control volumes with a stretch factor of 1.3. In the end, the following output are processed:

1. the hourly profile of temperature and relative humidity in the outer side of the insulation layer. A previous work demonstrated that this is the critical point for the mold growth in the investigated wall assembly (Urso et al, 2022);
2. the hourly moisture content, calculated as the average value in each layer.

On the one hand, from the first type of output it is possible to evaluate the mold growth risk according to VTT mold model (Ojanen et al, 2010). This allows to quantify the risk of mold formation by means of the Mold Index (MI), ranging between 0 (no mold growth) to 6 (very heavy and tight mold growth); MI = 3 is the risk threshold suggested by the authors. The model considers also the sensitivity to mold growth of materials. In the case of wood fiber, the type of material and surface is set to “sensitive”, and the type of mold growth is set to “almost no regression”. On the other hand, the second output can be used to evaluate the moisture-dependent thermal conductivity according to the following formula (Vogelsang et al, 2013):

$$\lambda(\theta) = \lambda_{\text{dry}} + 0.56 \cdot \text{MC} \quad (1)$$

Here, MC is the moisture content in the material layer ($\text{m}^3 \cdot \text{m}^{-3}$) and λ_{dry} is the thermal conductivity ($\text{W} \cdot \text{m}^{-1} \cdot \text{K}^{-1}$) of the material in dry conditions. Then, the increased heat losses due to moisture content are determined by comparing the moisture-dependent U-value, U_{wet} (i.e. calculated with the moisture-dependent thermal conductivity for each layer “i”), and the U-value in dry conditions, U_{dry} (i.e. calculated with the dry thermal conductivity for each layer “i”):

$$U_{\text{wet}} = \left[\frac{1}{h_{0,e}} + \sum_{i=1}^n \frac{s_i}{\lambda_i(\text{MC})} + \frac{1}{h_{0,i}} \right]^{-1} \quad (2)$$

$$U_{\text{dry}} = \left[\frac{1}{h_{0,e}} + \sum_{i=1}^n \frac{s_i}{\lambda_{\text{dry},i}} + \frac{1}{h_{0,i}} \right]^{-1} \quad (3)$$

In Eq. (2) and Eq. (3), $h_{0,e}$ and $h_{0,i}$ are respectively the outside and inside heat transfer coefficient previously defined, and “n” is the number of layers.

Results

This section compares the results of the simulations based on the three selected MRYs and the TWY, by looking at the Mould Index (MI) and the increase in the U-value due to the moisture retained in the wooden materials. All results refer to the tenth simulated year.

As a first result, Figure 3 shows the hourly trend of the MI in the outer side of the insulation layer, which has been identified as the critical point of the wall assembly. The East orientation is the one that implies the highest risk in terms of mould growth, and the simulations suggest that using the “COLD” MRY actually ensures reaching the highest MI values, meaning that it is suitable for conservative simulations. Nevertheless, the MI never exceeds $\text{MI} = 1$, and this means that all weather datasets imply a risk well below the critical threshold identified in the VTT model ($\text{MI} = 3$). In practice, even if the typical year implies lower MI values than MRY, this is not relevant considering that both datasets ensure the same degree of mould risk.

Based on these results, the moisture content (MC) inside the building materials is also likely not to significantly change with the various climate datasets. For this reason, Figure 4 reports the hourly trend of the MC in the CLT layer and in the insulation layer, i.e. the layers with the highest thermal resistance and the highest moisture storage capacity. The average volumetric MC in the CLT layer ranges between 4.8% and 5.2% during the year. The profile based on TWY is between the “HOT” and the “RAINY” profile. Instead, the average MC in the insulation layer ranges between 0.7% and 1.4%. Here, the profiles based on the different climate datasets almost overlap. Table 3 also collects the mean annual MC values: although the differences are not considerable, in this case the highest MC emerges with the “HOT” MRY dataset. The mean annual volumetric MC is 5.13% in the CLT layer and 1.11% in the insulation layer, and the difference with the results ensured by the TWY is only around 1%.

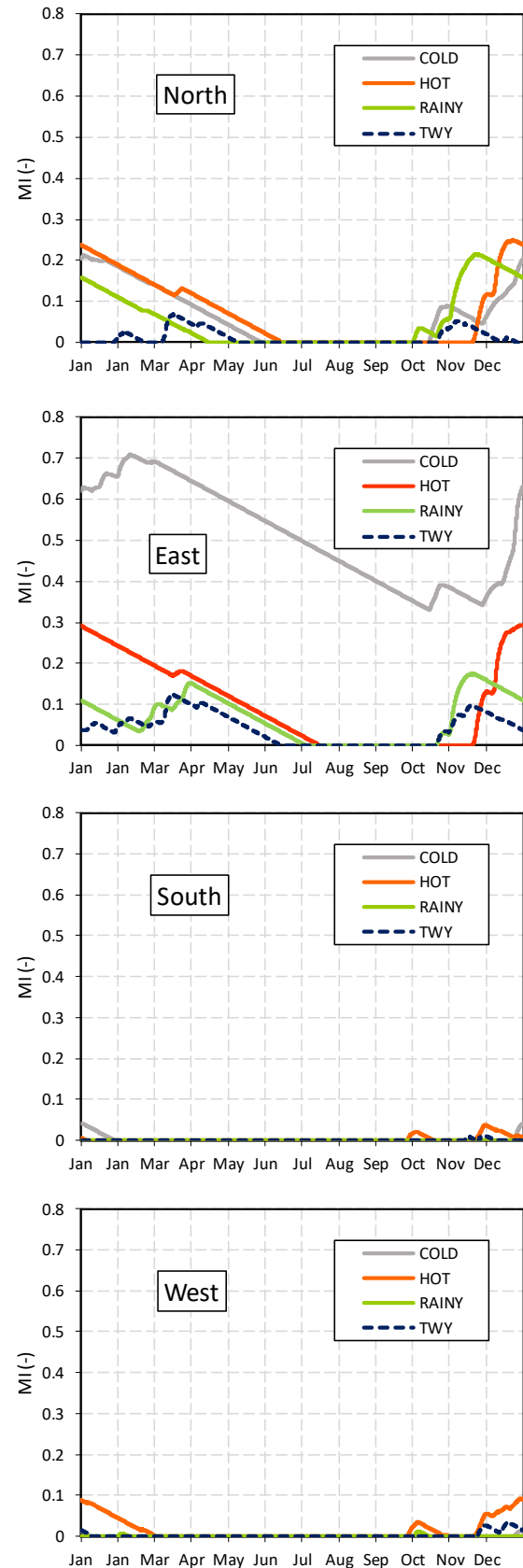


Figure 3: Time trend of the Mould Index associated with the various weather datasets, for different orientations.

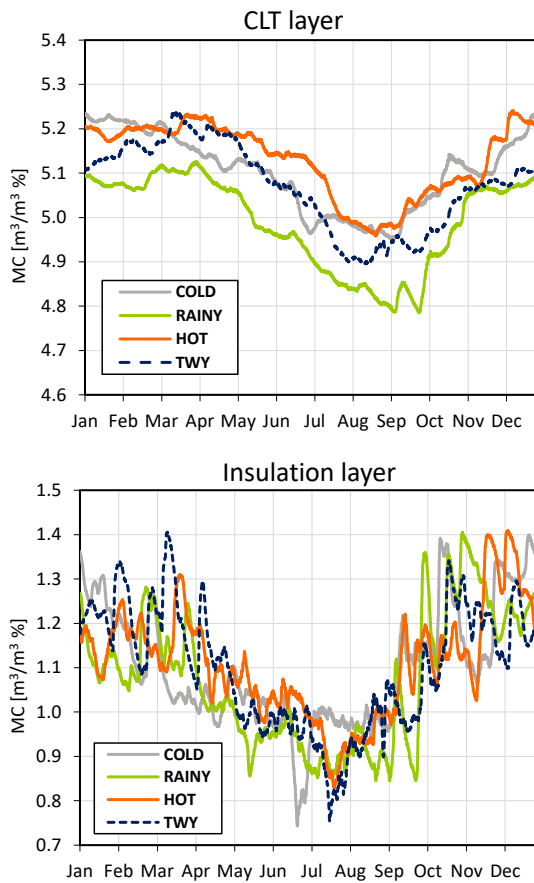


Figure 4: Time trend of the Moisture Content in the CLT and the wood fiber

Table 3: Mean annual values of the Moisture Content in the CLT and the wood fiber

	CLT layer (m ³ /m ³ %)			
	COLD	RAINY	HOT	TWY
North	5.10	4.99	5.13	5.07
East	5.05	4.88	5.01	5.00
South	4.91	4.81	5.00	4.91
West	4.93	4.87	5.04	4.93

	Insulation layer (m ³ /m ³ %)			
	COLD	RAINY	HOT	TWY
North	1.10	1.07	1.11	1.10
East	1.10	1.04	1.07	1.09
South	1.03	1.00	1.06	1.03
West	1.03	1.03	1.09	1.05

Finally, Figure 5 shows the mean annual increase in the wall thermal transmittance for each climate dataset and wall orientation here investigated. Coherently with the above results referring to the MC, the MRY which ensures the most conservative results in terms of increased U-value is the “HOT” one, in case of North orientation. However, in all cases, the discrepancies coming from the use of different climate datasets is not significant, as the variation in the U-values ranges from about 11% to about 12%, compared to the dry value. In particular, the

maximum U-value reached by the TWY is 0.3251 W/(m²·K), while the maximum U-value reached by the hot MRY is 0.3254 W/(m²·K). Such a small difference has emerged in this specific case study, featuring a warm climate. Different results might emerge in cold climates, which will be further elaborated in the Discussion.

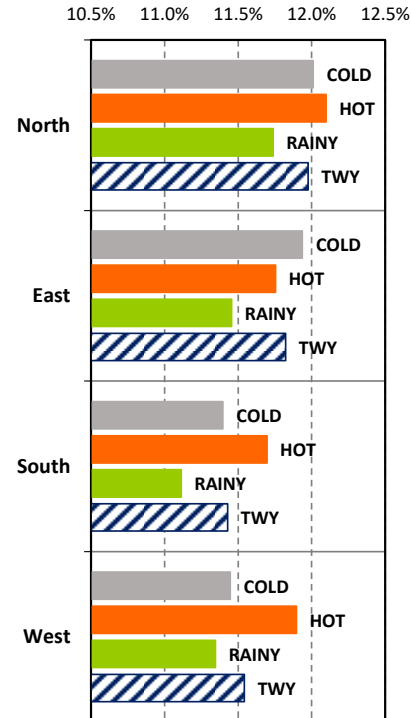


Figure 5: Percentage increase in the U-value of the investigated assembly, compared to dry conditions

Discussion

According to the results presented so far, and as far as the mold growth is concerned, the investigated wall is always mold-free, independently on the climate dataset and the wall orientation. This suggests that the use of a TWY in place of an MRY can be justified, at least in the warm climate of Catania and for the investigated wall typology. However, different results might emerge in different, and especially colder, climates. Then in order to better understand the results of the simulations and provide a more general view, a regression analysis is performed. In particular, the correlations between the maximum MI and, in turn, outdoor air temperature, relative humidity and wind driven rain is investigated.

Figure 6 reports the correlation between the monthly mean temperature and the monthly maximum MI. It refers only to the COLD and HOT weather datasets, which showed a similar but more evident linear correlation than with the other datasets ($R^2 = 0.870 - 0.887$ for the wall faced North, $R^2 = 0.710 - 0.876$ for the wall faced East). The scatter plot proves that the maximum MI tends to decrease with the increase in the mean monthly outdoor temperature: in other terms, higher air temperatures determine lower mold risk. This may justify the use of the “COLD” dataset as the worst MRY to evaluate the mold growth risk, while excluding the use of the “HOT” year.

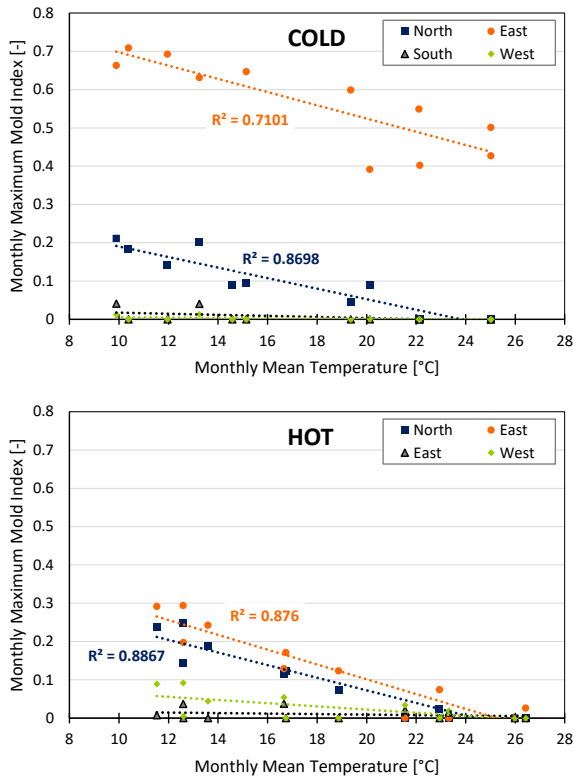


Figure 6: Correlation between monthly mean outdoor temperature and monthly maximum Mold Index.

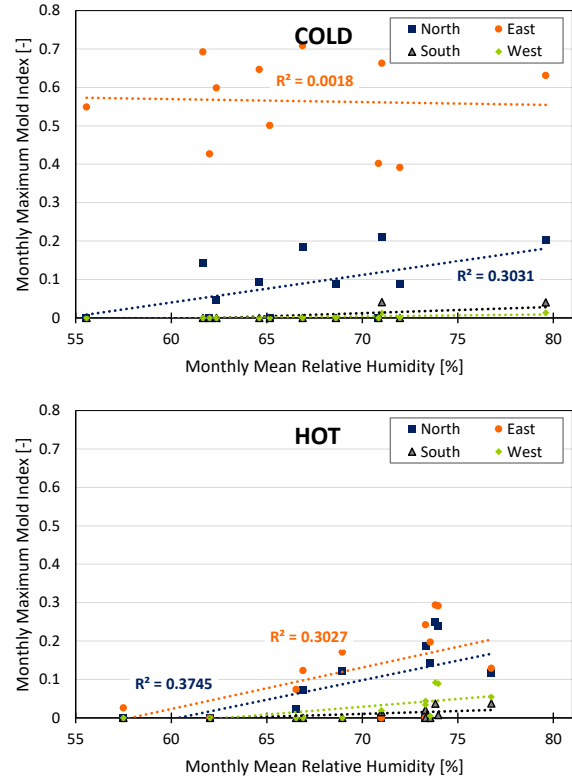


Figure 7: Correlation between monthly mean outdoor relative humidity and monthly maximum Mold Index.

Furthermore, the linear trend is very similar for all the wall orientations and climate years, thus forming a bundle of almost parallel lines. This suggests that the slope mainly depends on the temperature, while the maximum annual MI value depends on a climate variable related to the specific year and wall orientation, e.g. the WDR. Then, Figure 7 reports the correlation between the monthly mean relative humidity and the monthly maximum MI. Once again, only the “COLD” and “HOT” MRY datasets are reported. In this case, a certain increase in the maximum MI with the RH is observed, but the correlation is weak. Finally, the correlation between the yearly total WDR and the yearly maximum MI is shown in Figure 8. Here, the yearly parameters are preferred to better catch the long-term process of rain penetration inside the wall. In order to enlarge the number of points in the plot, thus finding a more significant correlation, the simulations are performed for each year of the reference period (2005 – 2019) and for each wall orientation. As expected, the WDR increases the mold growth risk. The dependency is polynomial and quite evident ($R^2 = 0.750$), according to Eq. (4):

$$\text{Max MI} = 0.0004 \cdot \text{WDR}^2 - 0.013 \cdot \text{WDR} + 0.1367 \quad (4)$$

Regarding the increased heat losses due to the moisture content within building materials, the results demonstrate that this is not clearly correlated with the climate dataset and the wall orientation. This suggests that a TWY is expected to be appropriate also to evaluate the impact of the moisture on building energy performance, even in colder and more humid climates.

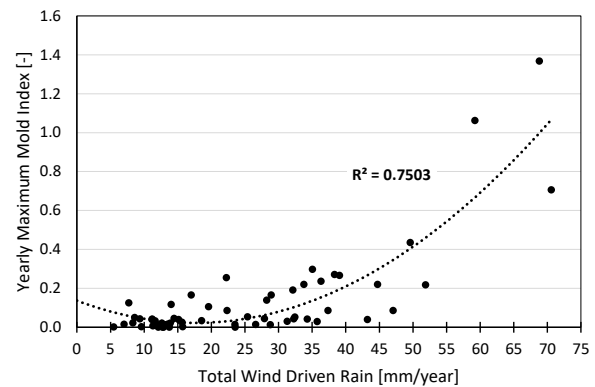


Figure 8: Correlation between total annual Wind Driven Rain and annual maximum Mold Index.

Conclusions

According to this study, the use of different “representative” weather years referred to the same location and reference period does not generate relevant discrepancies in the evaluation of moisture-related risks, such as mold growth and increased heat losses. Apart from small differences, all simulated cases show a MI well below the critical threshold, and an increased U-value ranging between 11% and 12%, compared to dry conditions. This can justify the use of available and easily accessible Typical Weather Years (TWY) in place of Moisture Reference Years (MRY) in the assessment of moisture-related risk, although they are not built *ad hoc* for hygrothermal simulations. This outcome refers to a warm climate where mold growth potential is not outstanding, so they cannot be extended a priori to other

colder climatic conditions, where the choice of the weather file might be more influential. For this reason, further investigations were made in the Discussion, showing that the maximum MI seems to be clearly correlated to the mean monthly outdoor temperature and the total annual Wind Driven Rain on the façade. The correlations identified in this paper may help understand to what extent a TWY and an MRY are likely to provide different results, based on how different the average values of the above weather parameters are.

Acknowledgements

This research was carried out in the framework of the e-SAFE project ("Energy and seismic affordable renovation solutions"), which has received funding from the European Union's Horizon 2020 Research and Innovation programme under Grant Agreement No. 893135. Neither the Executive Agency for Small-and-Medium-sized Enterprises (EASME) nor the European Commission is in any way responsible for any use that may be made of the information it contains. The activities are also partially funded by the University of Catania in the framework of the SIS-RENEW research project (Piano di incentivi per la Ricerca 2020–2022).

Nomenclature

Acronyms

CLT	Cross Laminated Timber
HAMT	Heat, Air and Moisture Transfer
IWEC	International Weather for Energy Calculations
MRY	Moisture Reference Year
SIAS	Sicilian Agrometeorological Information System
TWY	Typical Weather Year
VTT	Technical Research Centre of Finland
WF	Wood fiber
WPM	Water-proof membrane

Symbols

A	Water uptake coefficient ($\text{g}\cdot\text{m}^{-2}\cdot\text{s}^{-1/2}$)
c_p	Specific heat ($\text{J}\cdot\text{kg}^{-1}\cdot\text{K}^{-1}$)
$h_{0,i}$	Internal heat transfer coefficient ($\text{m}^2\cdot\text{K}\cdot\text{W}^{-1}$)
$h_{0,e}$	External heat transfer coefficient ($\text{m}^2\cdot\text{K}\cdot\text{W}^{-1}$)
MC	Moisture content (m^3/m^3)
MI	Mold index (-)
s_d	Equivalent air thickness (m)
s	Thickness (m)
U_{dry}	Dry thermal transmittance ($\text{W}\cdot\text{m}^{-2}\cdot\text{K}^{-1}$)
U_{wet}	Wet thermal transmittance ($\text{W}\cdot\text{m}^{-2}\cdot\text{K}^{-1}$)
λ_{dry}	Dry thermal conductivity ($\text{W}\cdot\text{m}^{-1}\cdot\text{K}^{-1}$)
μ	Vapor diffusion resistance factor (-)
ρ	Density ($\text{kg}\cdot\text{m}^{-3}$)
θ_{80}	Mass moisture content at RH = 80% ($\text{kg}\cdot\text{m}^{-3}$)
θ_{sat}	Mass moisture content at RH = 100% ($\text{kg}\cdot\text{m}^{-3}$)

References

ASHRAE (2016). ASHRAE Standard 160-2016. Criteria for Moisture-Control Design Analysis in Buildings (ANSI Approved).

Aversa, P., Marzo, A., Tripepi, C., Sabbadini, S., Dotelli, G., Lauriola, P., and V.A.M. Luprano (2021). Hemp-

lime buildings: thermo-hygrometric behaviour of two case studies in North and South Italy. *Energy and Buildings* 247, 111147.

- Brambilla, A., and E. Gasparri (2021). Mould growth models and risk assessment for emerging timber Envelopes in Australia: a comparative study. *Buildings* 11(6), 261.
- CEN, European Committee for Standardization (2007). *Hygrothermal performance of building components and building elements - Assessment of moisture transfer by numerical simulation* (EN ISO 15026:2007).
- CEN, European Committee for Standardization (2009). *Hygrothermal performance of buildings - Calculation and presentation of climatic data - Part 3: Calculation of a driving rain index for vertical surfaces from hourly wind and rain data* (EN ISO 15927-3).
- Chang, S.J., Yoo, J., Wi S., and S. Kim (202). Numerical analysis on the hygrothermal behavior of building envelope according to CLT wall assembly considering the hygrothermal-environmental zone in Korea. *Environmental Research* 191, 110198.
- Costanzo, V., Evola, G., Infantone, M., and L. Marletta (2020). Updated Typical Weather Year for the energy simulation of buildings in Mediterranean climate. A case study for Sicily. *Energies* 13, 4115.
- Delphin®, Version 6.1.2 (2021). Bauklimatik Dresden, Dresden, Germany. Available at: <https://bauklimatik-dresden.de/delphin/index.php>.
- Evola, G., Costanzo, V., and L. Marletta (2021). Hygrothermal and acoustic performance of two innovative envelope renovation solutions developed in the e-SAFE project. *Energies* 14(13), 4006.
- Evola, G., Costanzo, V., Urso, A., Tardo, C., and L. Margani (2022). Energy performance of a prefabricated timber-based retrofit solution applied to a pilot building in Southern Europe. *Building and Environment* 222, 109442.
- Evola, G., Urso, A., Costanzo, V., Nocera, F., and L. Marletta (2022). Heat and mass transfer modelling for moisture-related risks in walls retrofitted by timber materials. *Proceedings from BSA 2022: 5th Building Simulation Applications Conference. Bolzano (Italy), 30 June – 01 July 2022*.
- Koh, C.H.A., and D. Kraniotis (2021). Hygrothermal performance, energy use and embodied emissions in straw bale buildings. *Energy and Buildings* 245, 111091.
- Martín-Garín, A., Millán-García, J.A., Terés-Zubiaga, J., Oregi, X., Rodríguez-Vidal, I., and A. Bãiri (2021). Improving energy performance of historic buildings through hygrothermal assessment of the envelope. *Buildings* 11(9), 410.
- Ojanen, T., Viitanen, H., Peuhkuri, R., Lähdesmäki, K., Vinha, J., and K. Salminen (2010). Mold growth modeling of building structures using sensitivity classes of materials. *Proceedings from ASHRAE*

Buildings XI Conference. Clearwater Beach, Florida (USA), 5-9 December 2010.

Strang, M., Leardini, P., Brambilla, A., and E. Gasparri (2021). Mass timber envelopes in Passivhaus buildings: designing for moisture safety in hot and humid Australian climates. *Buildings 11(10)*, 478.

Urso A., Costanzo V., Nocera F., and G. Evola (2022). Moisture-related risks in wood-based retrofit solutions in a Mediterranean climate: design recommendations. *Sustainability 14*, 14706.

Vogelsang, S., Fechner, H., and A. Nicolai (2013). Delphin 6 material file specification, Version 6.0. Technical

report. Institut für Bauklimatik Technische Universität Dresden, Dresden, Germany.

Wang, L., Wang, J., and H. Ge (2020). Wetting and drying performance of cross-laminated timber related to on-site moisture protections: Field measurements and hygrothermal simulations. *Proceedings from E3S Web of Conferences, Yogyakarta (Indonesia), 7-8 September 2020.*

Zhu, N., Li, X., Hu, P., Lei, F., Wei, S., and W. Wang (2022). An exploration on the performance of using phase change humidity control material wallboards in office buildings. *Energy 239*, 122433